Involvement of Protein Kinase Cε (PKCε) in Thyroid Cell Death

A TRUNCATED CHIMERIC PKCε CLONED FROM A THYROID CANCER CELL LINE PROTECTS THYROID CELLS FROM APOPTOSIS*

Jeffrey A. Knauf‡, Rosella Elisei‡, Daria Mochly-Rosen§, Tamar Liron§, Xiao-Ning Chen¶, Rivkah Gonsky‖, Julie R. Korenberg¶, and James A. Fagin‡**

From the ‡Division of Endocrinology and Metabolism, University of Cincinnati, Cincinnati, Ohio 45267-0547, the §Department of Molecular Pharmacology, Stanford University, School of Medicine, Stanford, California 94025, the ‖Division of Endocrinology and Metabolism, and the ¶Department of Pediatrics, Medical Genetics Birth Defects Center, Cedars-Sinai Medical Center and UCLA School of Medicine, Los Angeles, California 90048

The protein kinase C (PKC) family has been implicated in the regulation of apoptosis. However, the contribution of individual PKC isozymes to this process is not well understood. We reported amplification of the chromosome 2p21 locus in 28% of thyroid neoplasms, and in the WRO thyroid carcinoma cell line. By positional cloning we identified a rearrangement and amplification of the PKCε gene, that maps to 2p21, in WRO cells. This resulted in the overexpression of a chimeric/truncated PKCε (Tr-PKCε) mRNA, coding for N-terminal amino acids 1–116 of the isozyme fused to an unrelated sequence. Expression of the Tr-PKCε protein in PCCL3 cells inhibited activation-induced translocation of endogenous PKCε, but its kinase activity was unaffected, consistent with a dominant negative effect of the mutant protein on activation-induced translocation of wild-type PKCε and/or displacement of the isozyme to an aberrant subcellular location. Cell lines expressing Tr-PKCε grew to a higher saturation density than controls. Moreover, cells expressing Tr-PKCε were resistant to apoptosis, which was associated with higher Bcl-2 levels, a marked impairment in p53 stabilization, and dampened expression of Bax. These findings point to a role for PKCε in apoptosis-signaling pathways in thyroid cells, and indicate that a naturally occurring PKCε mutant that functions as a dominant negative can block cell death triggered by a variety of stimuli.

Protein kinase C (PKC)[1] isozymes are involved in signal transduction pathways controlling growth, differentiation, and apoptosis (1, 2). In addition, PKCs are the major cellular receptors for the tumor promoter phorbol esters and related compounds. Because of this, there has been considerable interest in the potential role of PKC isozymes in the multistage process of carcinogenesis. However, isolating the role of the individual isozymes has proven to be complex due to apparent similarity in their substrate specificity, at least *in vitro*, as well as overlapping sensitivity to activators and inhibitors.

The PKC gene family is divided into three subgroups based on sequence homology and cofactor requirements: conventional PKC (α, βI, βII, and γ) which are dependent on Ca^{2+} for activation, nonconventional PKCs (δ, ϵ, η, and θ) that are not dependent on Ca^{2+} for activation, and atypical PKCs (ζ, λ/ι) which are not stimulated by diacylglycerol or phorbol esters and are Ca^{2+} independent (3). Cell signal pathways involving the PKC family are initiated by binding of a ligand to its respective cell surface receptor, which triggers the breakdown of phospholipids by phospholipase C and D producing many products including diacylglycerol (3, 4). Diacylglycerol binds to and activates most PKC isozymes, which then relocate to specific subcellular compartments that vary between the PKC isozymes as well as between cell types (5, 6). This relocation results from distinct protein-protein interactions, many of which are likely to be isozyme specific. Jaken, Scott, and collaborators (7–12) have identified talin, vinculin, a myristoylated protein kinase C substrate, a β-adducin homolog, AKAP79, as well as gravin/AKAP250 as PKC-associated proteins that require phosphatidylserine for binding. The binding of diacylglycerol is believed to lead to activation and relocalization of the PKCs through conformational changes that expose the catalytic domain as well as the region involved in binding to the docking site after translocation. This docking site has been termed RACK (receptor for activated C kinase), and each isozyme has been postulated to have its own specific RACK (6, 13), which is thought to determine the specific cellular location of the activated PKC isozymes. This property has been exploited for the past few years to develop isozyme-specific competitive antagonists (for review, see Ref. 14).

In a previous report (15) we describe the use of comparative genomic hybridization to detect regions of allelic imbalance in thyroid tumors, including an amplification event on chromosome 2p21 in 28% of the thyroid neoplasms examined, as well as in the clonal thyroid carcinoma cell line WRO. Positional cloning and sequencing of a BAC mapping to the 2p21 amplicon identified a candidate gene, protein kinase Cε (PKCε), which was amplified in the WRO cell line. Here we extended the analysis of this genetic event by describing that the PKCε gene was not only amplified, but also rearranged in the WRO cells. This complex genetic aberration leads to the overexpression of a chimeric and truncated PKCε (Tr-PKCε). The Tr-PKCε protein reported here is nearly identical to an N-terminal PKCε

[1] The abbreviations used are: PKC, protein kinase C; RACK, receptor for activated C kinase; Tr-PKCε, truncated PKCε; TSH, thyrotropin; BAC, bacterial artificial chromosome; PCR, polymerase chain reaction; PBS, phosphate-buffered saline; PAGE, polyacrylamide gel electrophoresis; RACE, rapid amplification of cDNA ends; kb, kilobase(s); MTT, 3-(4,5-dimethylthiazol-2-yl)-2,5-diphenyltetrazolium bromide; PMA, phorbol 12-myristate acetate.

fragment which has been demonstrated to specifically inhibit both activation-induced translocation of wild-type PKCϵ to its intracellular binding site as well as the biological effects mediated by this enzyme (16–18). We provide evidence that this truncated gene product interferes with the function of the wild-type isozyme in clonal thyroid cell lines and results in significant alterations in growth and apoptosis. In addition, we show that the inhibition of apoptosis in cells expressing Tr-PKCϵ is associated with impairment of the expected stabilization of p53 induced by DNA damage, and of the consequent activation of Bax. These data indicate that PKCϵ is involved in apoptosis signaling in thyroid cells, and raise the possibility that that loss of expression or function of PKCϵ may participate in thyroid tumorigenesis by inhibiting programmed cell death.

EXPERIMENTAL PROCEDURES

Cell Lines and Tissue Sample Collection

The human thyroid carcinoma cell lines NPA, ARO, and WRO were a gift of G. Juilliard (UCLA), and propagated in RPMI 1640 medium containing 10% fetal calf serum, non-essential amino acids (Irvine Scientific, Irvine, CA), glutamine (286 mg/liter), penicillin, and streptomycin (Life Technologies, Inc., Gaithersburg, MD), as described (19). PCCL3 cells were propagated in H6 medium, which consisted of Coons modification of Ham's F-12 media (Irvine Scientific, Irvine, CA) containing 5% fetal calf serum, glutamine (286 mg/l), somatostatin (10 ng/ml), glycyl-L-histidyl-L-lysin acetate (10 ng/ml), transferrin (5 μg/ml), hydrocortisone (10 nM), insulin (10 μg/ml), thyroid stimulating hormone (TSH, 10 mIU/ml), penicillin, and streptomycin, as described (20).

Demonstration of 2p21 Amplification in WRO Cells by FISH

WRO cell chromosome preparations were hybridized with the indicated bacterial artificial chromosome (BAC) clone as described previously (21). Briefly, the indicated BACs were biotin-labeled and hybridized to chromosome slides made from the WRO cell line. The images were captured using a Photometrics cooled-CCD camera (CH250) and Oncor image analysis system equipped with a Zeiss 135 Axovert fluorescence microscope.

Southern and Northern Blot Analysis

Southern blots of 10 μg of genomic DNA from the indicated sources digested with either *Eco*RI or *Bam*HI were performed as described (15). Membranes were probed with either the full-length (2.2 kb) human PKCϵ cDNA obtained by *Nhe*I digestion of the PKCϵ/pBluebac expression vector (22) or PCR products generated from the indicated regions of PKCϵ cDNA. Probes were labeled with [^{32}P]dCTP by random priming (Stratagene, San Diego, CA). Northern blots of 20 μg of total RNA were performed as described (23, 24) and hybridized with a full-length human [^{32}P]dCTP-labeled PKCϵ cDNA.

Total Cell lysates and Cell Fractionation

After washing, cells were scraped from the plate in ice-cold PBS and collected by centrifugation at 1000 $\times$ g for 10 min. The pellet was resuspended in buffer A (10 mM Tris-HCl, pH 7.5, 5.0 mM EDTA, 100 μg/ml phenylmethylsulfonyl fluoride, 4.0 mM EGTA, 1 μg/ml aprotinin, 5 μg/ml E-64, 1 μg/ml leupeptin, and 1 μg/ml pepstatin) containing 1% Triton X-100 and then lysed by passing through a 27-gauge needle 10 times. The lysate was then centrifuged at 10,000 $\times$ g for 15 min at 4 °C, the supernatant collected, and the protein concentration determined. Equal amounts of protein from each sample was then subjected to SDS-PAGE.

For preparation of soluble and particulate fractions the cells were homogenized in buffer B consisting of 50 mM Tris-HCl, pH 7.5, 5.0 mM EDTA, 100 μg/ml phenylmethylsulfonyl fluoride, 4.0 mM EGTA, 1 μg/ml aprotinin, 5 μg/ml E-64, 1 μg/ml leupeptin, and 1 μg/ml pepstatin by passing them through a 27-gauge needle 10 times. Soluble and particulate fractions were then separated by ultracentrifugation (100,000 $\times$ g for 1 h). The supernatant (soluble fraction) was removed and the pellet resuspended in buffer B with 1% Triton X-100. The Triton X-100-insoluble material was removed by centrifugation at 100,000 $\times$ g for 1 h and the supernatant collected (particulate fraction). The distribution of the PKC isozymes in the various fractions was then analyzed by Western blotting.

To better determine the distribution and relocation of PKCϵ after activation, PCCL3 cells were subfractionated into four parts as follows.

The cells were washed and scraped from the plate in ice-cold PBS. The cells were then washed with ice-cold buffer A and collected by centrifugation. The cell pellet was then resuspended in buffer A and the mixture incubated on ice for 10 min, passed through a 27-gauge needle 10 times, and the nuclei pelleted by centrifugation at 1000 $\times$ g for 10 min. The supernatant was removed and centrifuged at 100,000 $\times$ g at 4 °C for 60 min. The resulting supernatant (fraction F1, cytosol) was collected and the pellet resuspended in buffer A with 1% Triton X-100. The resuspended pellet was centrifuged at 100,000 $\times$ g at 4 °C for 60 min and the resulting supernatant collected (fraction F2, particulate extract). The intact nuclei were lysed by resuspending them in buffer A containing 600 mM KCl and centrifuged at 100,000 $\times$ g at 4 °C for 60 min and the resulting supernatant collected (fraction F3, nucleoplasm). The pellet was resuspended in buffer A with 1.0% Triton X-100, centrifuged at 100,000 $\times$ g at 4 °C for 60 min, and the supernatant collected (fraction F4, Triton-soluble nuclear extract). To remove the KCl from F3, the proteins were precipitated by the addition of trichloroacetic acid to a final concentration of 2%. The precipitated proteins were collected by centrifugation and the pellet resuspended in buffer A. The protein concentration of all fractions was determined using the micro BCA reagent, as directed by manufacturer (Pierce, Rockford, IL).

Western Blot Analysis

The indicated amount of protein from total cell lysates or cellular fractions were subjected to SDS-PAGE and Western blotting as described (25, 26). Blots were hybridized with antibodies to the indicated proteins and then with their corresponding species-specific horseradish peroxidase-conjugated secondary IgG and visualized using the Supersignal CL-HRP system (Pierce) as directed by manufacturer.

Identification of Chimeric Tr-PKCϵ mRNA using 3' RACE

The 3' RACE reaction was performed as described in Frohman *et al.* (27), except that the 5' primer was specific for exon 1 of PKCϵ (TGC-CCTCAATGTGGACGACTC). In addition, the second round of PCR amplification was performed under the following conditions: 95 °C for 45 s, 60 °C for 30 s, and 72 °C for 3 min. The PCR products generated were cloned into the pCR-II vector by TA cloning, as directed by the manufacturer (InVitrogen, Carlsbad, CA). Cloned inserts that were confirmed to contain exon 1 of PKCϵ by Southern blot analysis were sequenced using an ABI 373 automatic sequencer.

Preparation and Screening of the WRO Cell cDNA Library

Poly(A)$^+$ RNA was isolated from the WRO cell line using a PolyATtract mRNA system (Promega, Madison, WI). cDNA was generated from poly(A)$^+$ RNA and then cloned into a λ expression vector using a ZAP Express Vector Kit (Stratagene, San Diego, CA). The λ cDNA library was then screened as directed by the manufacturer (Stratagene), using a probe labeled by random priming in the presence of [^{32}P]dCTP. The probe used was generated by PCR amplification of a clone obtained by 3' RACE (described above) which contained part of PKCϵ exon 1 (base 140–364) and a 3' end that did not correspond to either intron 1 or exon 2, and was thought to have resulted from a rearrangement of the PKCϵ gene. Positive plaques were isolated and the ExAssist helper phage (Stratagene) used to generate a recircularized pBK-CMV phagemid (Stratagene) containing the positive cDNA. DNA isolated from these clones were reconfirmed by Southern blotting to contain exon 1 of PKCϵ, and then sequenced using an ABI sequencing machine.

Generation of PKCϵ Expression Constructs

The expression construct containing the Tr-PKCϵ (amino acids 1–116) was obtained, as described above, from the *in vivo* excision of a clone isolated from the WRO cDNA library. The expression construct containing the V1 region of PKCϵ (amino acids 2–142 (16)) was a generous gift from Dr. Robert Messing (University of California, San Francisco) and has been previously described (17).

Generation of Tr-PKCϵ Stably Transfected Cell Lines

PCCL3 cells were plated (5 $\times$ 10^5 cells/35-mm dish) and grown at 37 °C with 5% CO$_2$. After 24 h the cells were transfected by LipofectAMINE-mediated gene transfer, as directed by the manufacturer (Life Technologies, Inc.). Briefly, 10 μl of LipofectAMINE were incubated with 1.0 μg of plasmid and 200 μl of serum-free medium for 30 min at room temperature. Then 800 μl of serum-free medium was added to the LipofectAMINE-plasmid mixture and the entire solution added to a plate which had been previously washed twice with PBS. Cells were incubated at 37 °C in 5% CO$_2$ for 5–8 h and the transfection
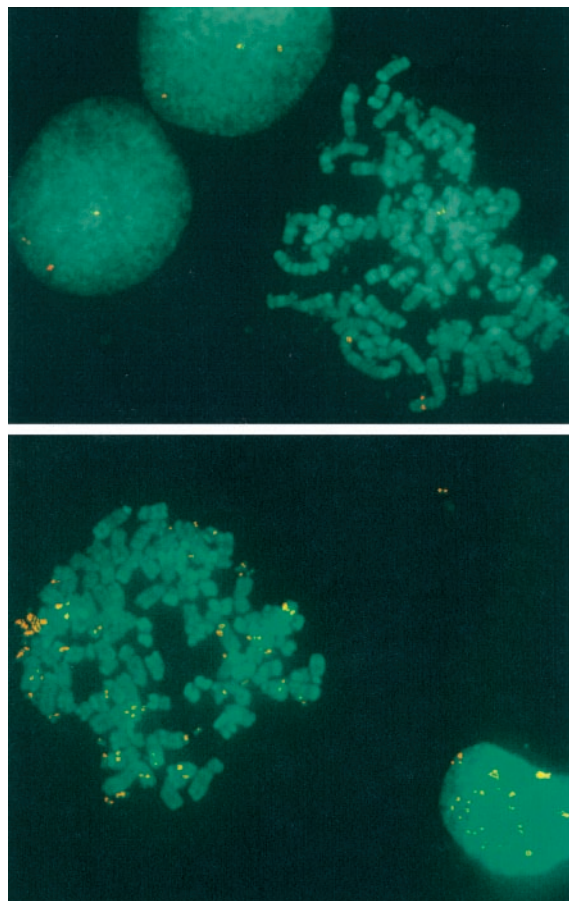
FIG. 1. **FISH of WRO chromosomes to BAC probes mapping to chromosome 2p21.** *Top,* BAC2B5 detects a single signal on each chromosome 2 (WRO cells are trisomic for this chromosome) in the metaphase shown. Three signals are also detected in the interphase nucleus. *Bottom,* BAC 1D9 shows a distinct pattern of amplification. In addition to the fluorescein isothiocyanate signals (*green spots*) detected on the three chromosome 2p21 loci, clusters of signals are detected on the multiple double minute chromosomes. Adjacent interphase nucleus also reveal multiple signals.

mixture replaced with H6 medium. After 24 h the cells were trypsinized and divided into four 100-mm dishes and single clones selected in H6 medium containing 300 μg/ml G418 (Life Technologies, Inc.). The mass-transfected lines were created as above except that after splitting into 100-mm dishes, individual G418 clones were not isolated, but instead, all G418-resistant colonies growing on that dish were pooled. Neomycin-resistant control cell lines were created by transfecting the pBK-CMV vector alone.

PKCε Immunofluorescence

Cells were plated into each of the four wells of a 4-well chamber-slide and incubated with H6 medium. When the cells became confluent, the medium was replaced by H6 medium with or without 100 nM PMA, and the cells incubated for 20 min at 37 °C with 5% CO_2. Cells were washed 3 times with ice-cold PBS and fixed by incubating the slides in 50:50 methanol/acetone at -20 °C for 4 min. Nonspecific interaction was blocked by a 30-min incubation in PBS containing 2 mg/ml bovine serum albumin, 10% goat serum, and 0.1% Triton X-100. Cells were then incubated in PBS containing 2 mg/ml bovine serum albumin, 5% goat serum, and polyclonal anti-PKCε IgG (Santa Cruz Biotechnology) for 16 h at 4 °C. The cells were washed with 3 sequential 5-min incubations in PBS containing 2 mg/ml bovine serum albumin, followed by a 2-h incubation at room temperature in PBS containing 2 mg/ml bovine serum albumin, 5% goat serum, and fluorescein isothiocyanate-conjugated goat anti-rabbit IgG (Jackson ImmunoResearch Laboratories, Inc., West Grove, PA). The slides were washed again 3 times and then mounted in Vectorshield (Vector Laboratories Inc., Burlingame, CA). They were viewed under a Zeiss Axiophot microscope. The images were captured onto Kodak 6400 ASA film using an MC100 camera.

PKCε Kinase Assay

Cells were washed and then scraped from the plate in ice-cold PBS, and collected by centrifugation at $1000 \times g$ for 10 min. The cell pellet was resuspended in extraction buffer (20 mM Tris-HCl, pH 7.5, 0.5% Nonidet P-40, 250 mM NaCl, 3 mM EDTA, 1 mM EGTA, 1 mM dithiothreitol, 2 mM Na_3VO_4, 25 μg/ml aprotinin, 25 μg/ml leupeptin, 100 μg/ml phenylmethylsulfonyl fluoride) and passed through a 27-gauge needle 10 times, and then centrifuged for 15 min at $10,000 \times g$ at 4 °C. The supernatant was collected and the protein concentration determined. Extracts were diluted into extraction buffer (final protein concentration 1 μg/μl) and added to 3 μg of rabbit anti-PKCε IgG (Santa Cruz Biotechnology, Inc., Santa Cruz, CA) which had been preincubated with protein G-agarose overnight at 4 °C. This mixture was then incubated for 4 h at 4 °C. The beads were then washed 3 times with PBS containing 0.1% Triton X-100 and then 3 times with kinase buffer (20 mM HEPES, pH 7.2, 137 mM NaCl, 5.4 mM NaH_2PO_4, 0.4 mM KH_2PO_4, 25 mM β-glycerophosphate, 10 mM $MgCl_2$, 0.5 mM EGTA, and 0.25 mM $CaCl_2$). Beads were resuspended in kinase buffer containing 0.013 μCi/μl [γ-^{32}P]ATP, 50 μM ATP, 125 ng/μl PKA inhibitor, and 0.4 mg/ml myelin basic protein and incubated at room temperature for 30 min. The reaction was stopped by adding SDS-PAGE loading buffer and then incubating at 95 °C for 5 min. The reaction was then size separated by 15% SDS-PAGE, transferred to a nylon membrane, and phosphorylation of the myelin basic protein quantitated by PhosphorImager analysis. Background was determined by substituting normal rabbit IgG for the rabbit anti-PKCε IgG.

Growth Curves

The plating efficiency (ratio of cells attached to cells plated) of each clone was determined by plating a known number of cells in H6 medium. The plate was incubated for 24 h at 37 °C in 5% CO_2 at which time the cells were detached by trypsinization and counted with a Z1 Coulter counter. Plating of each clone for growth curves was done in triplicate, after accounting for differences in plating efficiency, to obtain 50,000 cells per well of a 6-well plate after 24 h. The cells were grown in H6 medium with or without TSH at 37 °C in 5% CO_2. At the indicated times the cells were detached by trypsinization and counted using a Z1 Coulter counter.

Assays for Apoptosis

Cells grown in H6 medium were allowed to reach 95% confluency and then the medium replaced with fresh H6 medium containing the indicated amounts of actinomycin D or doxorubicin or alternatively cells were irradiated with the indicated dose of UV. Apoptosis was measured with the following methodologies.

DNA Fragmentation—Cells were incubated for the indicated times and the attached cells were collected by trypsinization then combined with the detached cells suspended in the medium. DNA was then extracted and 20 μg from each sample was electrophoresed through a 2% agarose-TBE gel and the DNA visualized by staining with ethidium bromide.

Cell Detachment—The cells were plated and grown as above. At the indicated times the number of cells in the medium was determined using a Z1 Coulter counter. More then 95% of detached cells examined by light microscopy after Diff-Quik staining or fluorescent microscopy after propidium iodide staining were found to have condensed and fragmented nuclei, consistent with death via apoptosis.

TUNEL Analysis—We also confirmed that cell death was via apoptosis by TUNEL analysis using the Apotag *In Situ* Apoptosis kit, as directed by the manufacturer (Oncor Inc., Gaithersburg, MD).

MTT Assay—To determine cell viability an MTT assay was performed as directed by the manufacturer (Sigma). Briefly, H6 medium was removed from cells and replaced with H6 medium containing 0.5 mg/ml 3-(4,5-dimethylthiazol-2-yl)-2,5-diphenyltetrazolium bromide (MTT) (Sigma-Aldrich, St. Louis, MO) and incubated for 2 h at 37 °C. The medium was removed and the colored precipitate formed by cleavage of MTT in living cells was solubilized with isopropyl alcohol containing 0.05 M HCl. Cell survival was determined by absorbance at 570 nm. Background was determined by absorbance at 660 nm.

Nude Mouse and Soft Agar Assays

Athymic nude/nude mice were purchased from Harlan Sprague-Dawley, Indianapolis, IN. For each cell line tested 1×10^6 cells in 200 μl of sterile PBS were injected into the right flank of 4 nude/nude mice. The animals were followed for 8 weeks with weekly inspection for nodules. To assay for anchorage-independent growth soft agar colony formation assays were performed by suspending 2×10^3 cells in 1.0 ml of 0.5%
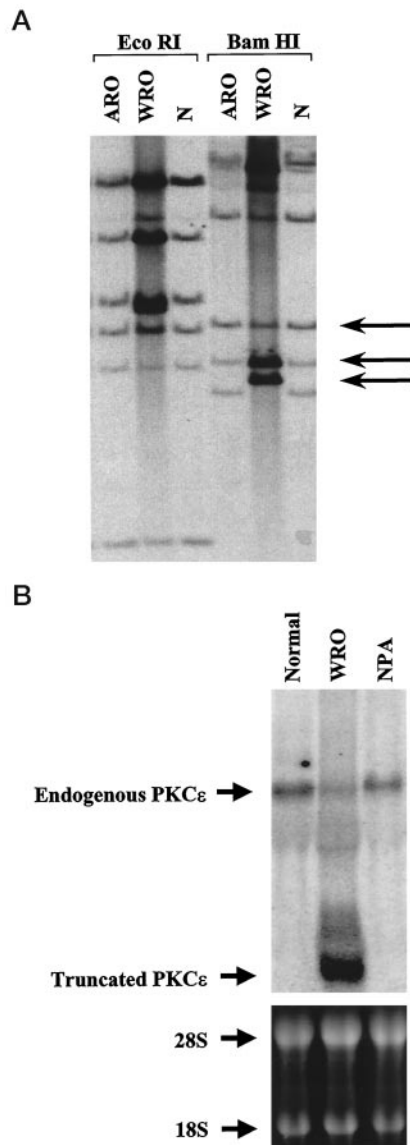
rived from a chromosome 2-specific library (15). One of these, BAC 1D9, was demonstrated by FISH analysis to be amplified 40–70 times in the WRO cell line (Fig. 1), a thyroid cancer cell line that contains double minute chromosomes. Sequencing of the entire BAC 1D9 demonstrated that it contained the first coding exon of the PKCε gene. Hybridization of the full-length human PKCε cDNA to Southern blots containing DNA from the WRO cell line, the anaplastic thyroid carcinoma cell line ARO, and normal tissue demonstrated that the PKCε gene has undergone rearrangement and amplification in the WRO cells, since there were additional bands found in the WRO cell line that were not found present in normal tissue or in ARO cells (Fig. 2). Furthermore, it is clear that only part of the PKCε gene is amplified in the WRO cells, as not all hybridizing bands were over-represented (Fig. 2). To map the location of the amplification and rearrangement, PCR products specific to different regions of the PKCε cDNA were generated and hybridized to Southern blots. This demonstrated that the 5′ break point of the internal deletion was between bases 366 and 599 of PKCε cDNA (data not shown), whereas hybridization with probes mapping to bases 1136–2244 showed that all were amplified, indicating that at least part of the 3′ end of the gene was within the amplicon. These Southern blot data suggest that the changes in the PKCε gene are a result of an internal deletion followed by an amplification of the rearranged gene.

To ascertain what effects the amplification and rearrangement of the PKCε gene has on its expression, Northern blots containing 20 μg of RNA from two clonal thyroid cancer cell lines and normal thyroid tissue were probed with the 2.2-kb PKCε cDNA (Fig. 2). Expression of the full-length PKCε mRNA was slightly lower in WRO, than in normal thyroid tissue. In addition, there was a PKCε hybridizing mRNA of approximately 2.2 kb in the WRO cell line, suggesting this cell line has an abnormal PKCε transcript. The identity of this mRNA was determined by sequencing products generated by 3′ RACE, and found to be a chimeric and truncated PKCε (Tr-PKCε) species that contained exon 1 of PKCε fused to an unrelated sequence.

To obtain the Tr-PKCε cDNA in its entirety, a WRO cDNA library was constructed and screened with the DNA product generated by 3′ RACE. Probing duplicate membranes from 5 plates, containing 30,000 plaques each, we identified more than 40 plaques that were positive in both membranes. The positive plaques were isolated and the corresponding pBK-CMV phagemids containing the Tr-PKCε cDNAs were generated by *in vivo* excision. Sequencing of 6 unique phagemids established that all the cDNAs contained exon 1 of PKCε spliced to 1 of 2 sequence fragments unrelated to PKCε. The non-PKCε sequences extended the PKCε reading frame by either 23 (found in 2/6 clones) or 2 amino acids (found in 4/6 clones) (Fig. 3*A*). The latter clone was chosen for all further studies since it was the most common. A search of GenBank, EST, and EMBL data bases revealed no significant homology of the non-PKCε sequences. Furthermore, these sequences were not part of the large >55-kb intron 1 sequenced from BAC 1D9. The conservation of exon 1 of PKCε (amino acids 1–116) between the different Tr-PKCε mRNAs suggests that this is likely to be the biologically relevant part of the message. This is further supported by the observation that a N-terminal fragment of PKCε (amino acids 2–142), corresponding to the V1 region of the protein (Fig. 3*B*), as well as a peptide derived from this fragment (amino acids 14–21), are capable of impairing PKCε function in PC12 cells (17) and cardiac myocytes (16, 28) by selectively inhibiting activation-induced translocation of PKCε.

To test whether the Tr-PKCε has similar properties in WRO cells, Western blots containing the soluble and particulate fraction from three different clonal thyroid cancer cell lines (ARO,

FIG. 2. **Southern and Northern blots of WRO cells.** *A,* Southern blot containing 10 μg of DNA from ARO and WRO cells and normal tissue, digested with *Eco*RI or *Bam*HI. The blots were hybridized with the full-length PKCε cDNA. Only some DNA bands from WRO cells are amplified. *Top arrow* points to a *Bam*HI band present at normal dosage. *Middle arrow* points to an amplified band of normal size. *Lower arrow* indicates an aberrantly sized amplified fragment, consistent with amplification of a rearranged PKCε gene in the WRO cell line. *B,* Northern blot containing 20 μg of total RNA from normal thyroid tissue, NPA cells, and WRO cells. *Top,* blot hybridized with the full-length PKCε cDNA. The *upper arrow* (~7.2 kb) indicates the position of the full-length PKCε mRNA and the *lower arrow* (~2.2 kb) indicates position of the Tr-PKCε mRNA. *Bottom,* ethidium bromide staining of the gel.

Bacto-agar (Difco Laboratories, Detroit, MI) in H6 medium, and overlaying the suspension in triplicate onto a layer of 2 ml of 0.6% Bacto-agar in H6 medium in each well of a 6-well plate. The cells were refed every 5th day by overlaying 1 ml of 0.5% Bacto-agar in H6 medium. After 20 days the colonies with more than 50 cells were counted.

RESULTS

Identification of a Chimeric PKCε in the WRO Cell Line—We have previously reported mapping of the PKCε gene to the 2p21 locus (15), a region found by comparative genomic hybridization to be amplified in 28% of thyroid neoplasms studied. The amplification was mapped to a series of BAC/PAC clones de-

A

```
TGGAGCTCGCGCGCCTGCAGGTCGACACTAGTGGATCCAAAGAATTCGGCACGAGCCGGGCGCGGCGCCC  70
GCTTTCCCGCAGTCCGGAGCCGGAGAGCCAGCGAGGCGGCGAGGCAGCCCCCGCGGCTTGCAGCGGAGCC 140
GACAGCTCGTCTTCTCTTCTGGAGGTGCAGCTGGTGGTCGGGGGGAGAGACTTGCTCCAAACACGGACAT 210
CCCCCAGTCTCTCCCCCTCCCTGTTTTCCGTTAGGAACCCGGCGAGGAAATACATGCACTGGCTGAGAA  280
TCGCCCCGCGCCAGGGCGCAACGCCACAAGGTGTAGGGAGTGTGCGGGGTGGGGCGAAAGGGGACCCAAGA350
GTCCTGTGGCTGGAGTGCCGGGCCGTCGGTTCTTCATTCCTGCCCTCGGGGCAGACGGAGTGACCCCG   420
GCCCCCACTCCCCGCCCCGACCATGGTAGTGTTCAATGGCCTTCTTAAGATCAAAATCTGCGAGGCCGTG 490
                       M  V  V  F  N  G  L  L  K  I  K  I  C  E  A  V
AGCTTGAAGCCCACAGCCTGGTCGCTGCGCCATGCGGTGGGACCCCGGCCGCAGACTTTCCTTCTCGACC 560
 S  L  K  P  T  A  W  S  L  R  H  A  V  G  P  R  P  Q  T  F  L  L  D
CCTACATTGCCCTCAATGTGGACGACTCGCGCATCGGCCAAACGGCCACCAAGCAGAAGACCAACAGCCC 630
 P  Y  I  A  L  N  V  D  D  S  R  I  G  Q  T  A  T  K  Q  K  T  N  S  P
GGCCTGGCACGACGAGTTCGTCACCGATGTGTGCAACGGACGCAAGATCGAGCTGGCTGTCTTTCACGAT 700
 A  W  H  D  E  F  V  T  D  V  C  N  G  R  K  I  E  L  A  V  F  H  D
GCCCCCATAGGCTACGACGACTTCGTGGCCAACTGCACCATCCAGTTTGAGGAGCTGCTGCAGAACGGGA 770
 A  P  I  G  Y  D  D  F  V  A  N  C  T  I  Q  F  E  E  L  L  Q  N  G
GCCGCCACTTCGAGGACTGGG *TTTTATGAGACCAGAGGTAATTCCCTGCTGCTGTTCAGCGTTGCTGTGG* 840
 S  R  H  F  D  W  V  L  ...
*CTAACAGTTCCAACCTTCTGAAGTGCCGGCTGGTTGGGGCTGTCTCTCTCGGCAACTGATTAGCCCATAAA* 910
*CCCTGCCTTGCTGGTCCTGCAGCCGTTCTCCAGTGCAAGTGACTGAAAGCATGCCTTTCCCAAAAAGGAAA* 980
*ATATGTAAGATTTAGTTCCCAAGTTATGTTTCATGTCTACAACGGTCTTCTCATCATCGTTAGTTGGATT* 1050
*ACAATTTACTGATTTCTCAC* 1070
```

```
*GGTGTGTGTGCCTGTAAGTCTCAGTTTCCTTGGGGAGGTACACTTCACTTCATAATTGGGGAAAAATAGG* 861
  G  V  C  A  C  K  S  Q  F  P  W  G  G  T  L  H  F  I  I  G  E  K  ...
*CATTGGCGACGAACATGACACTTGGAAAAAGGATGTGGCCCTCTGCTCCCCTCTGTGCCCTCCATTTGGT* 931
*GGGTGC* 937
```

B

FIG. 3. **Sequence and structure of a Tr-PKCε cloned from a WRO cell cDNA library.** *A,* the highlighted sequence is complimentary to the first coding exon of the PKCε gene (as inferred from the intron-exon boundary determined by sequencing genomic DNA from BAC 1D9). The additional sequence is unrelated and extends the open reading frame by 2 amino acids. **, indicates alternative fusion sequence which extends the reading frame by 23 amino acids. *B,* functional domains of the Wt-PKCε protein. The *bar* shown *below* represents the region of Wt-PKCε gene found in the Tr-PKCε. The *V* and *C* domains represent regions that are variable or conserved, respectively, between the different PKC isozymes. The *V1* region contains the site involved in the interaction of PKCε with its intracellular docking protein, β′-COP. The *V3* region contains the hinge domain and protease cleavage sites, both of which are thought to be important in regulating PKCε function. To date no specific function has been assigned to regions V4 and V5. The *C1* region contains the pseudosubstrate site and the phorbol ester and actin-binding sites. Region C3 contains the ATP-binding site and C4 contains the domain involved in phosphate transfer.
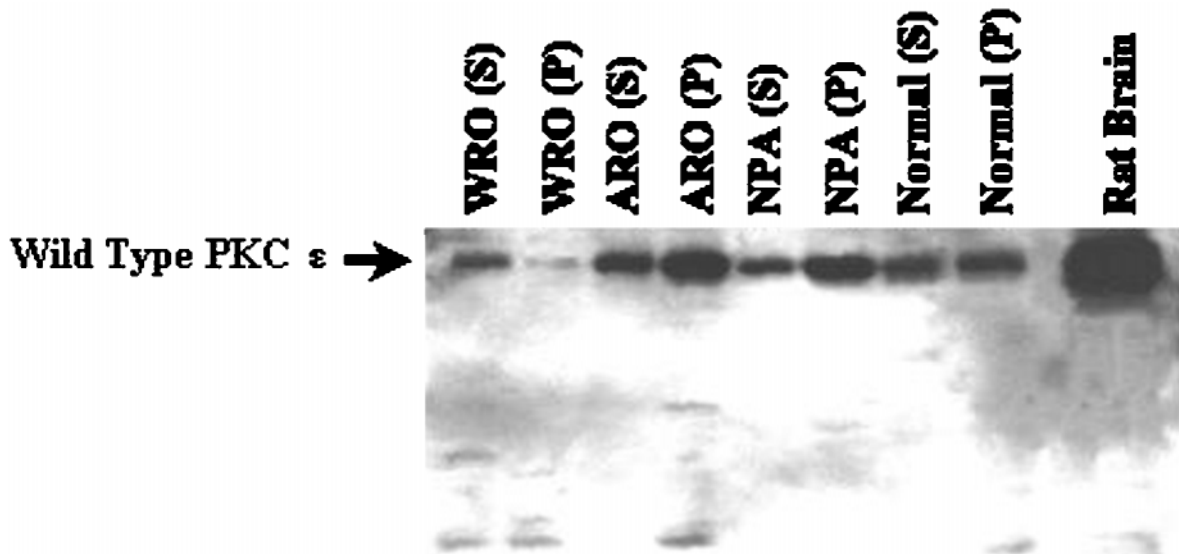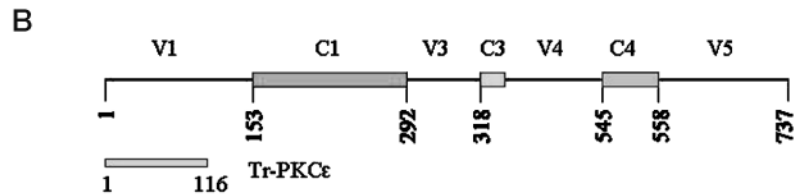

FIG. 4. **Western blot of PKCε in human thyroid carcinoma cell lines.** Thirty μg of protein from either the soluble (*S*) or particulate (*P*) fractions of the indicated cell lines or normal thyroid tissue were electrophoresed in a 7.5% SDS-PAGE and transferred to a nitrocellulose membrane. The blot shown is representative of two separate experiments. PKCε was detected using a rabbit polyclonal anti-PKCε IgG (Santa Cruz) and an horseradish peroxidase-conjugated goat anti-rabbit IgG. The *arrow* shows the position of the wild-type PKCε (~90 kDa).

NPA, and WRO) and normal thyroid tissue were probed with an anti-PKCε IgG. Whereas in normal thyroid tissue and the thyroid cancer cell lines ARO and NPA the majority of PKCε is found in the particulate fraction (52.4, 74.3, and 67.3%, respectively), in WRO cells only 22.3% was found in this compartment (Fig. 4). In addition, the total level of PKCε in the WRO cell line was 64% less than that in the other two cell lines. These observations are consistent with a role of the Tr-PKCε in preventing translocation after activation (16, 17, 28). Of note, the antibody used in the Western blots was generated against amino acids 722–726 of the isozyme, and was therefore not expected to recognize the Tr-PKCε or the V1 fragment (amino acids 2–142) of PKCε. In addition, none of the other commercially available antibodies have been demonstrated to recognize the V1 fragment.

Production of PCCL3 Cell Lines Overexpressing Tr-PKCε and the V1 Region of PKCε—To investigate the function of the Tr-PKCε, the pBK-CMV vector containing Tr-PKCε was stably
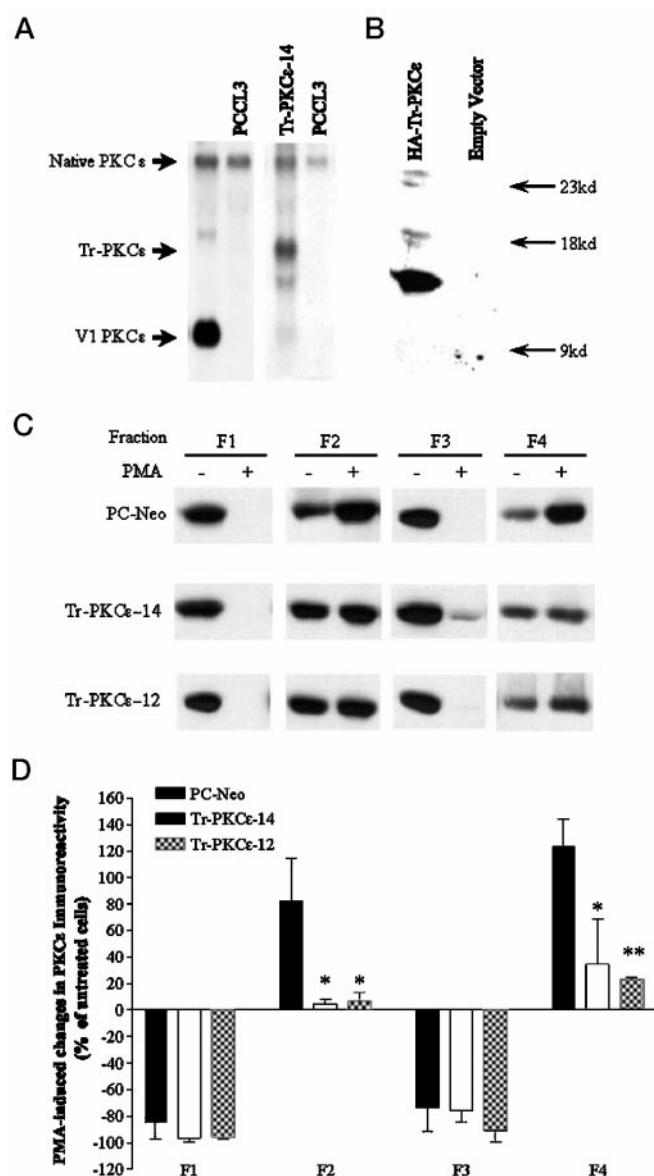
FIG. 5. **Expression of Tr-PKCϵ in PCCL3 cells and impact on PMA-induced PKC translocation.** *A,* Northern blots of 20 μg of total RNA from the indicated cell lines, probed with full-length PKCϵ cDNA. *B,* Western blot of PCCL3 cells stably transfected with pPK-RSV or pPK-RSV containing the HA-tagged Tr-PKCϵ. *C,* effects of Tr-PKCϵ expression on PMA-induced translocation of wild-type PKCϵ. Western blots of Neo-transfected or Tr-PKCϵ-transfected cells treated with or without 100 nM PMA for 20 min. Tr-PKCϵ-12 and -14 are clonal lines documented to stably express the mutant isozyme. Cells were harvested, and subjected to a 4-part fractionation. The level of PKCϵ in each fraction was determined by probing Western blots containing 30 μg of protein from each of the 4 fractions with rabbit polyclonal anti-PKCϵ IgG. *D,* the intensity of the PKCϵ band in each fraction was determined by densitometry and used to calculate the percent change in band intensity of PMA-treated *versus* untreated cells. The *bars* represent mean $\pm$ S.E. of three independent experiments. *, $p < 0.05$ *versus* PC-Neo; **, $p < 0.009$ *versus* PC-Neo.

transfected into PCCL3 cells, a well differentiated rat clonal thyroid cell line that is TSH-dependent for growth, iodide uptake, and expression of thyroglobulin and thyroid peroxidase. Twenty neomycin-resistant clones from Tr-PKCϵ transfections were isolated and screened for expression of the transfected product, resulting in 6 clones that expressed Tr-PKCϵ mRNA. PCCL3 cell lines were also mass transfected with a pRc-RSV expression vector containing the V1 fragment of the isozyme (amino acids 2–142), known to inhibit the translocation and

function of PKCϵ in rat cardiac myocytes (16), rat islet cells (18), and PC12 cells (17). Northern blots of the transfected cell lines probed with the various cDNAs demonstrated a 4–6-fold overexpression of the specific PKCϵ product compared with endogenous PKCϵ (Fig. 5*A*). Since no antibody to the V1 region of PKCϵ was available we also produced an HA-tagged Tr-PKCϵ cDNA construct and stably transfected it into PCCL3 to demonstrate appropriate expression of the Tr-PKCϵ protein (Fig. 5*B*).

Effect of Tr-PKCϵ on PMA-induced Relocation of Endogenous PKCϵ—To explore relocation of PKCϵ in PCCL3 cells, lysates were fractionated into four parts: F1, enriched for cytosol; F2, plasma membrane and organelles; F3, nucleoplasm; and F4, nuclear membrane. Endogenous PKCϵ in untreated, Neo-transfected cells is found mainly in F1 and F3 (Fig. 5, *C* and *D*). After treatment with PMA, the PKCϵ protein is no longer found in F1 and F3, and increases in the membrane-containing fractions F2 and F4. In PKCϵ-expressing cells PKCϵ is also almost fully displaced from F1 and F3 after PMA. However, there is no increase in F2 or F4 (Fig. 5, *C* and *D*). The presence of PKCϵ in fractions F2 and F4 in the Tr-PKCϵ cells under basal conditions may be the result of nonspecific or secondary anchoring sites that are unaffected by the Tr-PKCϵ, as suggested by Mayne and Murray (29), since they are not altered by treatment with PMA. It is possible that the mistranslocated PKCϵ is degraded, since we have found that activated PKCs are less stable if their translocation is inhibited (28).[2] To explore this possibility, total cell lysates were prepared from cells treated for 0–6 h with PMA. Western blots demonstrated similar levels of PKCϵ in both controls and Tr-PKCϵ-expressing cells during the first hour after PMA treatment (data not shown). These results indicate that the lack of appearance of PKCϵ in F2 and F4 was not due to degradation *in vivo*, since the fractionation experiment was performed in cells treated with PMA for only 20 min. The most likely explanation is that blocking interaction of PKCϵ with its RACK renders it more sensitive to nonspecific proteolysis during fractionation. Overexpression of PKCϵ-V1 resulted in similar effects (not shown). Of note, the PMA-induced translocation of PKCα and βI, and basal levels of PKCζ were unaffected in the Tr-PKCϵ expressing cells (not shown). PCCL3 cells had no detectable PKCβII, δ, γ, or η. The above results are consistent with a model by which Tr-PKCϵ inhibits interaction of activated wild-type PKCϵ with its RACK. In support of this conclusion, immunofluorescent staining of PCCL3 cells with anti-PKCϵ antibody demonstrated immunoreactivity distributed throughout the cytosol under basal conditions. Upon activation with PMA, PKCϵ localized to the plasma membrane as well as to perinuclear Golgi-like structures. However, in cell lines expressing the Tr-PKCϵ, PKCϵ did not localize to either the plasma membrane or the Golgi after PMA treatment (Fig. 6).

To determine the impact of translocation inhibition on the enzymatic function of PKCϵ, we measured the ability of immunoprecipitated PKCϵ to phosphorylate myelin basic protein *in vitro*. There was a 3-fold increase in myolin basic protein phosphorylation in both control cells and cells expressing the Tr-PKCϵ after activation with PMA (data not shown). This indicates that, as expected (6, 17), the Tr-PKCϵ does not modify PKCϵ kinase activity, but likely interferes with the function of its wild-type counterpart by displacing it to an inappropriate cell compartment after activation.

Effects of Overexpressing Tr-PKCϵ on Growth Rate and Saturation Density of PCCL3 Cells—Removal of TSH for 8 days resulted in a complete inhibition of growth in Neo-transfected

---

[2] D. Mochly-Rosen, unpublished results.

Untreated　　　**100 nM PMA**

FIG. 6. **Localization of PKCε by immunofluorescence in native PCCL3 and Tr-PKCε-14 cells.** PKCε localization was detected after incubation with a rabbit polyclonal anti-PKCε IgG and an fluorescein isothiocyanate-conjugated goat anti-rabbit IgG. *A,* untreated PCCL3 cells. *B,* PCCL3 cells treated with 100 nM PMA for 20 min. *C,* untreated Tr-PKCε cells. *D,* Tr-PKCε cells treated with 100 nM PMA for 20 min. The images shown (× 40 magnification) are representative of three independent experiments.
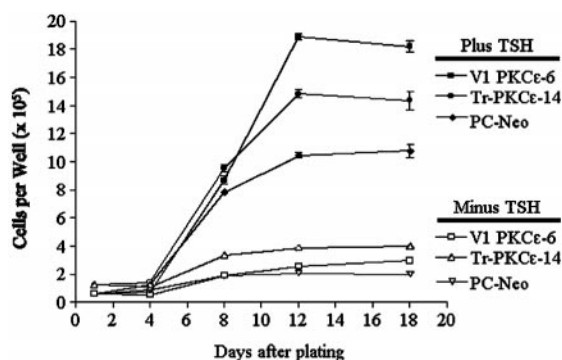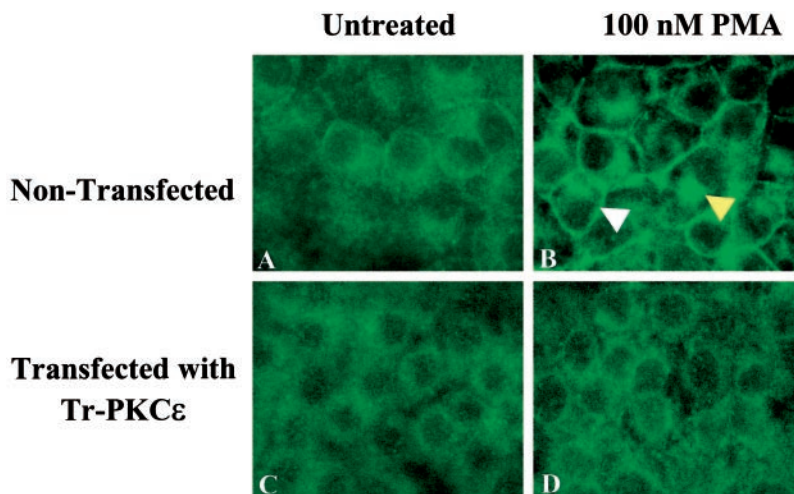

FIG. 7. **Growth curve of Neo-transfected PCCL3 and the indicated V1-PKCε or Tr-PKCε-overexpressing cell lines.** Data illustrate results of one experiment performed in triplicate, which was similar to those obtained in a second experiment. *Open* and *closed symbols* represent cell counts with or without 10 mIU/ml of TSH, respectively. Neo-transfected, Tr-PKCε, and V1-PKCε-transfected cells are indicated by *diamonds, circles*, and *squares*, respectively.

cells, as well as those expressing Tr-PKCε or V1-PKCε, indicating that expression of the PKCε fragments did not confer cells with TSH-independent growth. In the presence of TSH, Neo-transfected, Tr-PKCε, and V1-PKCε expressing cells had similar initial doubling times (22.9, 23.0, and 24.4 h, respectively) (Fig. 7). However, Tr-PKCε and V1-PKCε expressing cells grew to a higher saturation density than the Neo-transfected controls (Fig. 7).

Formation of Tumors in Nude Mice and Colonies in Soft Agar—To determine whether the Tr-PKCε products have transforming properties on PCCL3 cells, Tr-PKCε, or V1-PKCε-expressing cell lines were tested for colony formation in soft agar, and for ability to form subcutaneous tumors in athymic mice. Whereas the human thyroid carcinoma cell lines ARO, FRO, and WRO formed colonies in soft agar, neither PCCL3-Neo, Tr-PKCε-14, Tr-PKCε-12, nor V1-PKCε-expressing cells scored in the assay (not shown). Similarly, all mice injected with the human thyroid cancer cell lines developed tumors within 6 weeks (4/4 each), whereas the Neo control and Tr-PKCε expressing cells did not.

Effects of overexpression of Tr-PKCε on Apoptosis—Inhibition of macromolecular synthesis results in apoptosis in a variety of cell types (30), including the thyroid (31). To confirm that actinomycin D, an RNA synthesis inhibitor, was also able to induce apoptosis in the PCCL3 cells, they were incubated with various concentrations of actinomycin D for 24 h and the cells harvested. The DNA from the collected cells exhibited a dose-dependent increase in nucleosomal fragmentation, indicative of apoptosis (Fig. 8*A*). Furthermore, greater than 95% of the detached cells exhibited nuclear condensation or nuclear fragmentation as determined by Diffico blue staining or propidium iodide staining, respectively, confirming that cell detachment could be used as a quantitative indicator of apoptosis under these conditions. The above observations demonstrated that the incubation of PCCL3 cells with actinomycin D induces cell death via an apoptotic pathway.

To characterize the effects of overexpressing Tr-PKCε and V1-PKCε on apoptosis, the different cell lines were incubated with actinomycin D and the number of detached cells determined. Greater than 90% of the untransfected and Neo-transfected cells detached from the dish after 16 h of incubation with actinomycin D (Fig. 8*B*). In contrast, there was less than 20% detachment in cell lines overexpressing Tr-PKCε or V1-PKCε. The resistance of the cells expressing the Tr-PKCε or V1-PKCε to apoptosis was confirmed by TUNEL analysis (Fig. 8*C*) and DNA fragmentation (Fig. 8*D*). The protective effects of Tr-PKCε and V1-PKCε were also apparent when apoptosis was triggered through alternative mechanisms, such as exposure to UV irradiation or to doxorubicin (Fig. 9).

Effects of Overexpression of Tr-PKCε on p53—Doxorubicin has been reported to induce apoptosis via a p53-mediated mechanism (32). Indeed, doxorubicin increased p53 levels within 6 h in Neo-transfected PCCL3 cells, with maximal induction at 12 h (Fig. 10, *A* and *B*). By contrast there was only a slight increase in p53 after addition of doxorubicin in cell lines expressing the Tr-PKCε, suggesting that the mutant isozyme may inhibit DNA damage-induced activation of p53. As predicted, p53 mRNA was unchanged 6 h after addition of doxorubicin, and actually declined at 12 and 18 h (data not shown), demonstrating that the increase in p53 protein was a result of post-translational changes, most likely stabilization. MDM2, a nuclear protein induced by p53, binds to the p53 trans-activation domain and promotes its proteasome-mediated degradation (33, 34). After exposure to doxorubicin, MDM2 levels increased transiently in PCCL3-Neo cells, but did so more robustly and persistently in cell lines expressing Tr-PKCε (Fig. 10*A*). p53 has been reported to lead to apoptosis in part by its ability to transactivate expression of Bax (35, 36). In accordance with these reports, doxorubicin increased Bax protein levels in Neo-transfected PCCL3 cells, an effect that was markedly inhibited by expression of Tr-PKCε (Fig. 10, *A* and *C*). Finally, whereas doxorubicin decreased abundance of the anti-apoptotic factor Bcl-2 in both Neo- and Tr-PKCε-expressing cells, absolute levels of Bcl-2 were 2–5-fold higher in cells expressing the Tr-PKCε at all time points (Fig. 11). Of note,

FIG. 8. **Induction of apoptosis by actinomycin D.** *A,* PCCL3 cells grown in H6 medium were treated with the indicated concentration of actinomycin D for 24 h. At that time all attached and detached cells were combined and the DNA isolated. Twenty μg of DNA was then electrophoresed through a 2% agarose/TBE gel and the DNA detected by ethidium bromide staining. The 1-kb ladder (*far right lane*) indicates DNA laddering units of 180–200 base pairs, consistent with the nucleosomal fragmentation seen in apoptosis. *B,* the indicated cells were incubated with 1.0 μg/ml actinomycin D and the number of detached cells were determined by counting cells in the medium. The data shown is an average of a single experiment performed in triplicate and is similar to that obtained in two additional experiments. *C,* cells from the indicated lines were incubated with 1.0 μg/μl actinomycin D for 16 h, fixed with paraformaldehyde, and the extent of apoptosis determined by TUNEL analysis. The *bars* represent mean ± S.E. of an experiment performed in triplicate. *, $p < 0.0006$ *versus* PC-Neo. *D,* 20 μg of DNA isolated from cells incubated in H6 medium containing 1.0 μg/ml actinomycin D for the indicated times (h) was electrophoresed through a 2% agarose/TBE gel. The DNA was detected by staining with ethidium bromide. The data illustrated is representative of two separate experiments.
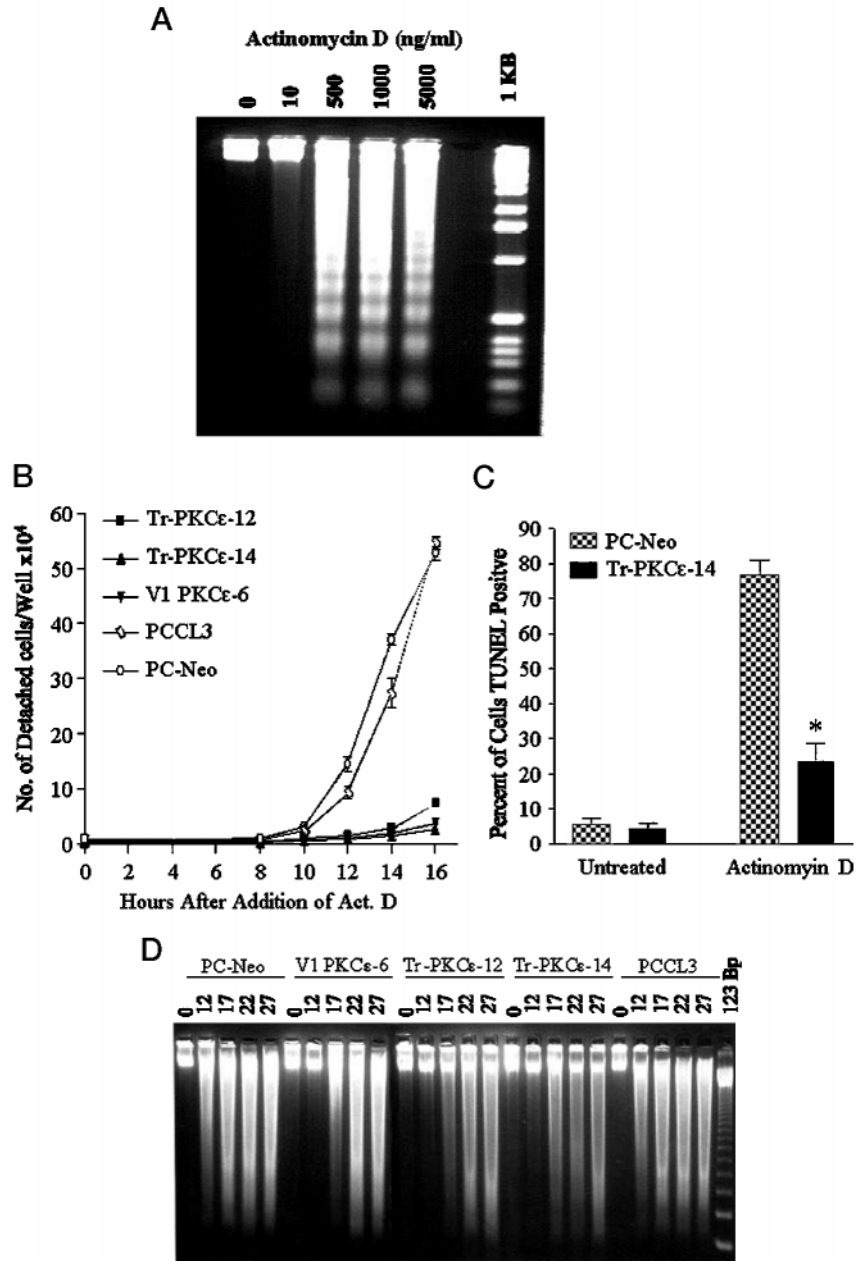
levels of Bcl-X$_L$, Bcl-X$_S$, or Bad were not affected by expression of the Tr-PKCε or treatment with doxorubicin (data not shown).

DISCUSSION

Whereas activation of PKCs is important in regulating cell proliferation, differentiation, and apoptosis of most cell types, the contribution of individual PKC isozymes in these processes is not well understood. Our interest in the function of PKCε in thyroid cells resulted from our characterization of a rearrangement and amplification of the PKCε gene in WRO thyroid carcinoma cells (15). This complex mutation was identified by positional cloning of a defect initially detected by comparative genomic hybridization, and as such, is to our knowledge the first previously unmapped candidate tumor-promoting gene uncovered with this methodology. The WRO cell line lacked identifiers, and it was not possible to determine whether the PKCε rearrangement was also present in the original tumor. Moreover, further manipulation of PKCε in this cell line is unlikely to be informative, since it has a number of other genetic defects including inactivating mutations of p53 and p16 (37, 38). The 2p21 amplicon gave rise to double minute chromosomes. The double minute chromosomes containing the rearranged PKCε gene have persisted through serial passaging for several years, despite the fact that double minute chromosomes are known to be unstable structures, suggesting that their presence conferred WRO cells with a selective advantage. As a result of this chromosomal abnormality, WRO cells display high level expression of a chimeric gene product, consisting of the first coding exon of the PKCε gene fused to one of two unrelated fragments, the most common of which codes for a 2 amino acid C-terminal tail. Exon 1 of PKCε codes for part of the V1 region of the protein, that contains the domain involved in the interaction of the activated isozyme with its intracellular docking protein(s) (16, 17, 28), one of which was recently identified as β'-COP (39).

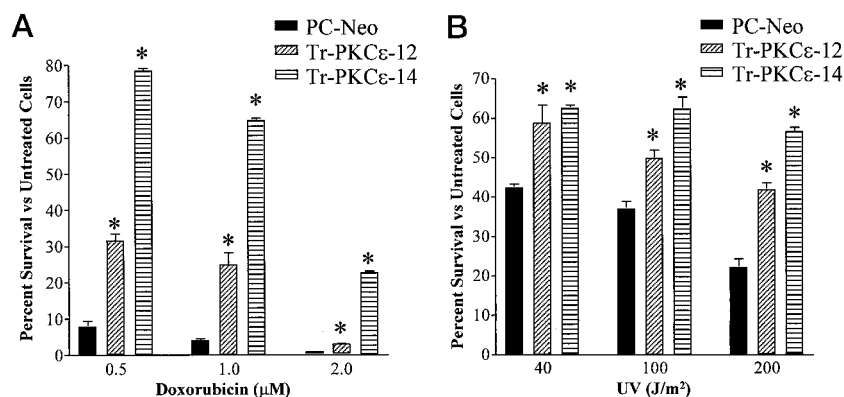A powerful approach to determine the role of individual PKC

Protein Kinase Cε and Thyroid Cell Apoptosis

FIG. 9. **Induction of apoptosis by doxorubicin and UV irradiation.** *A,* survival of the indicated cell lines treated with 0.5–2.0 μM doxorubicin at 37 °C for 48 h. The *bars* represent mean ± S.E. of two experiments performed in duplicate. *, $p < 0.0004$ *versus* PC-Neo. *B,* survival of the indicated cell lines irradiated with 40–200 J/m^2 and then incubated at 37 °C for 24 h. The *bars* represent mean ± S.E. of two experiments performed in duplicate. *, $p < 0.005$ *versus* PC-Neo. Cell survival was determined using an MTT assay. *Bars* represent the mean from three independent experiments.

isozymes is to specifically inhibit their function by preventing translocation and binding to their respective anchoring proteins (*i.e.* their isozyme-specific RACK) using peptides or protein fragments containing the domain involved in the interaction. This strategy has been used successfully to dissect the specific function of the classical PKC isozymes α and β (18, 40, 41), PKCε (16–18, 28, 29), and PKCδ (17) in different cell types. As there are no antibodies available that recognize the V1 region of PKCε, we could not directly verify the *in vivo* location of the Tr-PKCε. However, transfection of PCCL3 cells with an HA-tagged Tr-PKCε resulted in expression of a protein that was distributed throughout the cell, perhaps due to saturation of the anchoring protein. The following observations strongly suggest that Tr-PKCε interacts with a PKCε-specific RACK and antagonizes binding of activated wild-type PKCε. 1) The Tr-PKCε protein contains the domain demonstrated to be important in the binding of PKCε with β'-COP, a protein demonstrated to act as a PKCε-specific RACK in cardiomyocytes (16, 39). 2) Unlike other thyroid cells, where greater than 50% of the isozyme is in the particulate fraction, the majority of wild-type PKCε is found in the soluble fraction in WRO cells (*i.e.* not bound to its RACK). 3) Transfection of PCCL3 rat thyroid cells with a Tr-PKCε-expression vector (containing amino acids 1–116 of the wild-type isozyme) inhibits the PMA-induced translocation of PKCε to membrane fractions that contain the activated protein. Similar results were obtained in PCCL3 cells overexpressing the V1 fragment of PKCε (amino acids 2–142). 4) Translocation of wild-type PKCε to Golgi-like structures and plasma membrane after PMA treatment is not seen in cell lines expressing the Tr-PKCε, or the V1 region of PKCε. 5) Expression of Tr-PKCε had selective effects on the homologous wild-type enzyme, and did not affect the abundance or subcellular distribution of other PKC isozymes, consistent with experiments in PC12 cells (17) and cardiac myocytes (28) after overexpression of the V1 fragment of PKCε, or introduction of the V1 fragment by transient permeabilization (16).

Although we favor the interpretation that Tr-PKCε functions as a competitive antagonist of the activation-induced binding of the wild-type protein to its intracellular anchoring protein, we cannot exclude the possibility that it may also have other independent effects. For example, inhibiting the interaction of PKCε with its RACK, which has been demonstrated to bind the majority of the activated enzyme (13), may promote the association of PKCε with other proteins such as Raf (42), 14-3-3 proteins (43), caveolin (44), AKAP79 (8, 9), or actin (45, 46). Given that the kinase activity of PKCε is still intact in cells

expressing the Tr-PKCε, and that PKCs have a relatively relaxed substrate specificity, it is possible that the displaced PKCε may aberrantly phosphorylate alternative substrates, and thus disrupt their function. Whether the phenotype of cells containing Tr-PKCε is a result of a disruption in binding to RACK, or secondary effects on alternative substrates by the displaced kinase remains to be determined.

Cell lines expressing the V1-PKCε or Tr-PKCε grew to a higher saturation density, implying that wild-type PKCε may play a role in contact inhibition, or as a negative regulator of thyroid cell growth. Although this observation contrasts with published data that PKC activation stimulates thyroid cell growth (47, 48), the results are not mutually exclusive, since previous investigators used PKC activators and inhibitors that are not specific to an individual PKC isozyme. Thus, it is possible that their observations result from the activation or inhibition of PKC isozyme(s) other than PKCε, and that the outcome of activation of the latter was not apparent in the context of a more comprehensive stimulation of the whole PKC signaling repertoire.

Many reports have suggested a role for individual PKC isozymes in cell transformation (reviewed in Ref. 49). PKCs can exert both positive and negative effects on cell growth, depending on the isozyme and the cell type involved. Of all PKC isozymes, PKCε has proven to be the most consistently transforming when transfected into murine fibroblasts (50, 51). When overexpressed in rat 6 cells, PKCε evoked malignant transformation in the absence of treatment with phorbol esters. In the presence of 12-*O*-tetradecanoylphorbol-13-acetate, PKCε-transfected cells exhibited a rearranged actin cytoskeleton and were growth inhibited, probably due in part to interference of the overexpressed isozyme with the translocation and activation of other PKC isozymes. Overexpression of PKCε also results in transformation of colonic epithelial (52), but not rat hepatoma cells (53).

The most significant phenotypic change introduced by expression of Tr-PKCε or V1-PKCε was protection from apoptosis. Disruptions in cellular control of programmed cell death are now recognized as common events in tumorigenesis (54, 55), by creating a permissive environment for the accumulation of genetic damage. There is relatively scant information on the physiological signals that trigger apoptosis in thyroid cells. Growth factor or TSH deprivation and protein synthesis inhibitors can trigger apoptosis in thyrocytes (31). The role of interleukin-1β and Fas is more controversial (56, 57). Downstream of these initiating events are a variety of intermediates that

FIG. 11. **Effect of Tr-PKCε on expression of Bcl-2.** *A,* Western blot of Neo- or Tr-PKCε-transfected cells treated with 1.5 μM doxorubicin for the indicated time, probed with an anti-Bcl-2 IgG. *B,* the intensity of the Bcl-2 band at each time point was determined by densitometry. Data represent the relative change in band intensity of doxorubicin-treated *versus* untreated cells. The *bars* represent mean ± S.E. of three separate experiments. *, $p < 0.05$ *versus* PC-Neo.
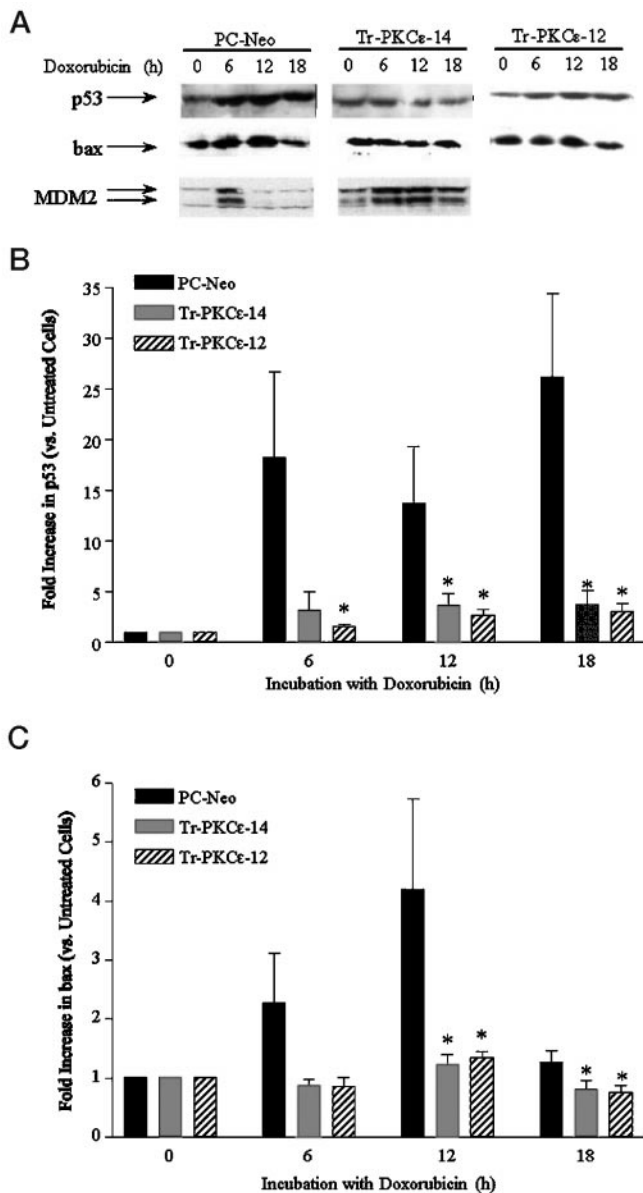
FIG. 10. **Effects of Tr-PKCε on induction of p53, Bax, and MDM2 after treatment with doxorubicin.** *A,* representative Western blot of Neo- or Tr-PKCε-transfected cells treated with 1.5 μM doxorubicin for the indicated time, probed with an anti-p53, anti-Bax, or anti-MDM2. *B,* the intensity of the p53 band at each time point was determined by densitometry. Data represent the relative change in band intensity of doxorubicin-treated *versus* untreated cells. The *bars* represent mean ± S.E. of three separate experiments. *, $p < 0.05$ *versus* PC-Neo. *C,* the intensity of the bax band at each time point was determined by densitometry. Data represent the relative change in band intensity of doxorubicin-treated *versus* untreated cells. The *bars* represent mean ± S.E. of three separate experiments. *, $p < 0.05$ *versus* PC-Neo.

has been reported to have diverse effects on programmed cell death, including both anti-apoptotic and pro-apoptotic effects (for review see, Refs. 1 and 60). Recent studies using strategies to explore the role of individual isozymes suggests that activation of PKCε may have a pro-apoptotic (61) or an anti-apoptotic (62) effect which is presumably dependent on cell type or apoptosis inducing agent. For example, down-regulation of PKCε and α by chronic exposure to a phorbol ester in human prostatic carcinoma cells was associated with resistance to VP-16- or melphalan-induced apoptosis. These effects were not abrogated in the presence of the PKC antagonist UCN-01 at concentrations that inhibited PKCα, but not PKCε, indirectly implicating the latter in the control of programmed cell death (61). By contrast, treatment with a peptide that inhibits PKCε-RACK interaction blunted the anti-apoptotic effect of PMA in U937 histiocytic lymphoma cells treated with TNFα (29). Furthermore, overexpression of wild-type PKCε in human TF-1 cells increased Bcl-2 expression and increased resistance to apoptosis induced by cytokine withdrawal (62).

Here we demonstrate that in PCCL3 cells doxorubicin induces p53 accumulation by a post-translational mechanism, and that this is inhibited by Tr-PKCε. Moreover, expression of Bax, a transcriptional target of p53, is also inhibited by the Tr-PKCε. UV radiation (63) and ceramide (64), a lipid second message commonly generated after DNA damage (65, 66), cause translocation of PKCε and ultimately apoptosis. These results suggest that DNA damage activates PKCε, and that this kinase is involved either directly or indirectly in stabilization and activation of p53. Disrupting the interaction of p53 with MDM2, which normally directs p53 for degradation via the proteasome, leads to an increase in stability of the p53 protein (for review, see Ref. 67). Moreover, this interaction is

either positively or negatively regulate apoptosis. The particular pathways used vary according to the cell type and the triggering event, and include, but are not limited to, signaling through the PKC and PKA families, hydrolysis of sphingomyelin, and activation of mitogen-activated protein kinase (for review, see Refs. 30, 58, and 59). We opted to explore the role of apoptosis by exposing cells to adverse conditions or well recognized DNA damaging agents: *i.e.* actinomycin D, UV irradiation, and doxorubicin. The protective effects of Tr-PKCε and V1-PKCε in response to these various treatments were consistent and of significant magnitude. Broad based PKC activation
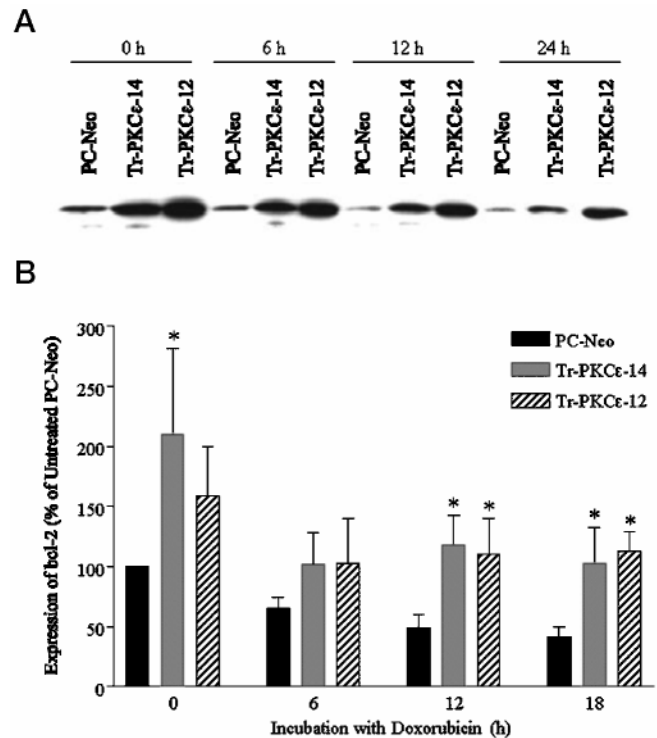
subject to regulation by proteins such as p300 (68, 69) and p19^ARF (for review, Ref. 70), as well as by phosphorylation of p53 (71) and/or MDM2 (72). Thus, it would be of future interest to determine the effects of Tr-PKCε, and thus of PKCε, on the factors that regulate the interaction of MDM2 with p53.

How may abnormalities of PKCε structure or function participate in the pathogenesis of human thyroid tumors? Activation of oncogenes such as *ras* (73–75) and *ret*/PTC (76, 77) are believed to be initiating events for tumors of thyroid follicular cells. The latter oncogene rearrangement is likely generated as a direct consequence of exposure to ionizing radiation (78, 79). However, *ras* mutations (80) and radiation exposure also activate apoptosis, and it is likely that for a tumor clone to progress the apoptotic program must be successfully disabled. This may occur through secondary mutations arising during tumor progression, or through epigenetic changes. A recent paradigm fitting this model is the recognition of genomic amplification of a decoy receptor for Fas ligand in colorectal and lung cancers (81). So far we have not detected rearrangements or amplification of PKCε in papillary carcinomas, or in a small subset of follicular carcinomas that we were able to examine (the tumor type from which WRO cells were derived). However, both papillary and follicular carcinomas have a high prevalence of isozyme-selective decreases in PKCε immunoreactivity as demonstrated by Western blotting, and of subcellular distribution revealed by immunohistochemistry, consistent with loss of function through alternative mechanisms that are yet to be defined.[3] We propose that functional compromise of PKCε by either genetic or epigenetic events may significantly threaten the ability of thyroid cells to respond appropriately to DNA damage, allowing them to escape an apoptotic fate, thus favoring tumor progression.

REFERENCES

1. Toker, A. (1998) *Front. Biosci.* **3,** D1134–1147
2. Lucas, M., and Sanchez-Margalet, V. (1995) *Gen. Pharmacol.* **26,** 881–887
3. Newton, A. C. (1997) *Curr. Opin. Cell Biol.* **9,** 161–167
4. Berridge, M. J., and Irvine, R. F. (1989) *Nature* **341,** 197–205
5. Goodnight, J., Mischak, H., Kolch, W., and Mushinski, J. F. (1995) *J. Biol. Chem.* **270,** 9991–10001
6. Mochly-Rosen, D. (1995) *Science* **268,** 247–251
7. Kiley, S. C., Jaken, S., Whelan, R., and Parker, P. J. (1995) *Biochem. Soc. Trans.* **23,** 601–605
8. Faux, M. C., and Scott, J. D. (1997) *J. Biol. Chem.* **272,** 17038–17044
9. Klauck, T. M., Faux, M. C., Labudda, K., Langeberg, L. K., Jaken, S., and Scott, J. D. (1996) *Science* **271,** 1589–1592
10. Hyatt, S. L., Liao, L., Chapline, C., and Jaken, S. (1994) *Biochemistry* **33,** 1223–1228
11. Hyatt, S. L., Liao, L., Aderem, A., Nairn, A. C., and Jaken, S. (1994) *Cell Growth Differ.* **5,** 495–502
12. Dell'Acqua, M. L., Faux, M. C., Thorburn, J., Thorburn, A., and Scott, J. D. (1998) *EMBO J.* **17,** 2246–2260
13. Mochly-Rosen, D., Khaner, H., and Lopez, J. (1991) *Proc. Natl. Acad. Sci. U. S. A.* **88,** 3997–4000
14. Souroujon, M. C., and Mochly-Rosen, D. (1998) *Nat. Biotechnol.* **16,** 919–924
15. Chen, X., Knauf, J. A., Gonsky, R., Wang, M., Lai, E. H., Chissoe, S., Fagin, J. A., and Korenberg, J. R. (1998) *Am. J. Hum. Genet.* **63,** 625–637
16. Johnson, J. A., Gray, M. O., Chen, C. H., and Mochly-Rosen, D. (1996) *J. Biol. Chem.* **271,** 24962–24966
17. Hundle, B., McMahon, T., Dadgar, J., Chen, C. H., Mochly-Rosen, D., and Messing, R. O. (1997) *J. Biol. Chem.* **272,** 15028–15035
18. Yedovitzky, M., Mochly-Rosen, D., Johnson, J. A., Gray, M. O., Ron, D., Abramovitch, E., Cerasi, E., and Nesher, R. (1997) *J. Biol. Chem.* **272,** 1417–1420
19. Zeki, K., Spambalg, D., Sharifi, N., Gonsky, R., and Fagin, J. A. (1994) *J. Clin. Endocrinol. Metab.* **79,** 1317–1321
20. Fusco, A., Berlingieri, M. T., Di Fiore, P. P., Portella, G., Grieco, M., and Vecchio, G. (1987) *Mol. Cell. Biol.* **7,** 3365–3370
21. Korenberg, J. R., and Chen, X. N. (1995) *Cytogenet. Cell Genet.* **69,** 196–200
22. Burns, D., Strickland, M., Holmes, W., Loomis, C., and Ballas, L. (1992) *Biochim. Biophys. Acta* **1134,** 154–160
23. Church, G. M., and Gilbert, W. (1985) *Prog. Clin. Biol. Res.* **177,** 17–21
24. Gonsky, R., Knauf, J. A., Elisei, R., Wang, J. W., Su, S., and Fagin, J. A. (1997) *Nucleic Acids Res.* **25,** 3823–3831
25. Laemmli, U. K. (1970) *Nature* **227,** 680–685
26. Towbin, H., Staehelin, T., and Gordon, J. (1979) *Proc. Natl. Acad. Sci. U. S. A.* **76,** 4350–4354
27. Frohman, M. A., Dush, M. K., and Martin, G. R. (1988) *Proc. Natl. Acad. Sci. U. S. A.* **85,** 8998–9002
28. Gray, M. O., Karliner, J. S., and Mochly-Rosen, D. (1997) *J. Biol. Chem.* **272,** 30945–30951
29. Mayne, G. C., and Murray, A. W. (1998) *J. Biol. Chem.* **273,** 24115–24121
30. Vaux, D. L., and Strasser, A. (1996) *Proc. Natl. Acad. Sci. U. S. A.* **93,** 2239–2244
31. Dremier, S., Golstein, J., Mosselmans, R., Dumont, J. E., Galand, P., and Robaye, B. (1994) *Biochem. Biophys. Res. Commun.* **200,** 52–58
32. Srivastava, R. K., Srivastava, A. R., Korsmeyer, S. J., Nesterova, M., Cho-Chung, Y. S., and Longo, D. L. (1998) *Mol. Cell. Biol.* **18,** 3509–3517
33. Haupt, Y., Maya, R., Kazaz, A., and Oren, M. (1997) *Nature* **387,** 296–299
34. Kubbutat, M. H., Jones, S. N., and Vousden, K. H. (1997) *Nature* **387,** 299–303
35. Miyashita, T., Krajewski, S., Krajewska, M., Wang, H. G., Lin, H. K., Liebermann, D. A., Hoffman, B., and Reed, J. C. (1994) *Oncogene* **9,** 1799–1805
36. Miyashita, T., and Reed, J. C. (1995) *Cell* **80,** 293–299
37. Elisei, R., Shiohara, M., Koeffler, H. P., and Fagin, J. A. (1998) *Cancer* **83,** 2185–2193
38. Fagin, J. A., Matsuo, K., Karmakar, A., Chen, D. L., Tang, S. H., and Koeffler, H. P. (1993) *J. Clin. Invest.* **91,** 179–184
39. Csukai, M., Chen, C. H., De Matteis, M. A., and Mochly-Rosen, D. (1997) *J. Biol. Chem.* **272,** 29200–29206
40. Zhang, Z. H., Johnson, J. A., Chen, L., El-Sherif, N., Mochly-Rosen, D., and Boutjdir, M. (1997) *Circ. Res.* **80,** 720–729
41. Ron, D., Luo, J., and Mochly-Rosen, D. (1995) *J. Biol. Chem.* **270,** 24180–24187
42. Cacace, A. M., Ueffing, M., Philipp, A., Han, E. K., Kolch, W., and Weinstein, I. B. (1996) *Oncogene* **13,** 2517–2526
43. Acs, P., Szallasi, Z., Kazanietz, M. G., and Blumberg, P. M. (1995) *Biochem. Biophys. Res. Commun.* **216,** 103–109
44. Oka, N., Yamamoto, M., Schwencke, C., Kawabe, J., Ebina, T., Ohno, S., Couet, J., Lisanti, M. P., and Ishikawa, Y. (1997) *J. Biol. Chem.* **272,** 33416–33421
45. Prekeris, R., Hernandez, R. M., Mayhew, M. W., White, M. K., and Terrian, D. M. (1998) *J. Biol. Chem.* **273,** 26790–26798
46. Prekeris, R., Mayhew, M. W., Cooper, J. B., and Terrian, D. M. (1996) *J. Cell Biol.* **132,** 77–90
47. Fujimoto, J., and Brenner-Gati, L. (1992) *Endocrinology* **130,** 1587–1592
48. Hoelting, T., Tezelman, S., Siperstein, A. E., Duh, Q. Y., and Clark, O. H. (1993) *Biochem. Biophys. Res. Commun.* **195,** 1230–1236
49. Goodnight, J., Mischak, H., and Mushinski, J. F. (1994) *Adv. Cancer Res.* **64,** 159–209
50. Cacace, A. M., Guadagno, S. N., Krauss, R. S., Fabbro, D., and Weinstein, I. B. (1993) *Oncogene* **8,** 2095–2104
51. Mischak, H., Goodnight, J., Kolch, W., Martiny-Baron, G., Schaechtle, C., Kazanietz, M. G., Blumberg, P. M., Pierce, J. H., and Mushinski, J. F. (1993) *J. Biol. Chem.* **268,** 6090–6096
52. Perletti, G. P., Folini, M., Lin, H. C., Mischak, H., Piccinini, F., and Tashjian, A. H. J. (1996) *Oncogene* **12,** 847–854
53. Perletti, G., Tessitore, L., Sesca, E., Pani, P., Dianzani, M. U., and Piccinini, F. (1996) *Biochem. Biophys. Res. Commun.* **221,** 688–691
54. King, K. L., and Cidlowski, J. A. (1995) *J. Cell. Biochem.* **58,** 175–180
55. Wright, S. C., Zhong, J., and Larrick, J. W. (1994) *FASEB J.* **8,** 654–660
56. Giordano, C., Stassi, G., De Maria, R., Todaro, M., Richiusa, P., Papoff, G., Ruberti, G., Bagnasco, M., Testi, R., and Galluzzo, A. (1997) *Science* **275,** 960–963
57. Arscott, P. L., Knapp, J., Rymaszewski, M., Bartron, J. L., Bretz, J. D., Thompson, N. W., and Baker, J. R. J. (1997) *Endocrinology* **138,** 5019–5027
58. Rowan, S., and Fisher, D. E. (1997) *Leukemia* **11,** 457–465
59. Schwartzman, R. A., and Cidlowski, J. A. (1993) *Endocr. Rev.* **14,** 133–151
60. Lavin, M. F., Watters, D., and Song, Q. (1996) *Experientia* **52,** 979–994
61. Rusnak, J. M., and Lazo, J. S. (1996) *Exp. Cell Res.* **224,** 189–199
62. Gubina, E., Rinaudo, M. S., Szallasi, Z., Blumberg, P. M., and Mufson, R. A. (1998) *Blood* **91,** 823–829
63. Zhuang, S., Hirai, S., Mizuno, K., Suzuki, A., Akimoto, K., Izumi, Y., Yamashita, A., and Ohno, S. (1997) *Biochem. Biophys. Res. Commun.* **240,** 273–278
64. Sawai, H., Okazaki, T., Takeda, Y., Tashima, M., Sawada, H., Okuma, M., Kishi, S., Umehara, H., and Domae, N. (1997) *J. Biol. Chem.* **272,** 2452–2458
65. Billis, W., Fuks, Z., and Kolesnick, R. (1998) *Recent. Prog. Horm. Res.* **53,** 85–93
66. Bose, R., Verheij, M., Haimovitz-Friedman, A., Scotto, K., Fuks, Z., and Kolesnick, R. (1995) *Cell* **82,** 405–414
67. Prives, C. (1998) *Cell* **95,** 5–8
68. Grossman, S. R., Perez, M., Kung, A. L., Joseph, M., Mansur, C., Xiao, Z. X., Kumar, S., Howley, P. M., and Livingston, D. M. (1998) *Mol. Cell* **2,** 405–415
69. Thomas, A., and White, E. (1998) *Genes Dev.* **12,** 1975–1985
70. Chin, L., Pomerantz, J., and DePinho, R. A. (1998) *Trends Biochem. Sci.* **23,** 291–296
71. Shieh, S. Y., Ikeda, M., Taya, Y., and Prives, C. (1997) *Cell* **91,** 325–334
72. Mayo, L. D., Turchi, J. J., and Berberich, S. J. (1997) *Cancer Res.* **57,** 5013–5016
73. Lemoine, N. R., Mayall, E. S., Wyllie, F. S., Farr, C. J., Hughes, D., Padua, R. A., Thurston, V., Williams, E. D., and Wynford-Thomas, D. (1988) *Cancer Res.* **48,** 4459–4463
74. Suarez, H. G., du Villard, J. A., Severino, M., Caillou, B., Schlumberger, M., Tubiana, M., Parmentier, C., and Monier, R. (1990) *Oncogene* **5,** 565–570
75. Namba, H., Gutman, R. A., Matsuo, K., Alvarez, A., and Fagin, J. A. (1990) *J. Clin. Endocrinol. Metab.* **71,** 223–229
76. Fabien, N., Paulin, C., Santoro, M., Berger, N., Grieco, M., Galvain, D., Bar-

[3] J. A. Knauf, T. Liron, W. Niu, D. Mochly-Rosen, and J. A. Fagin, unpublished data.

bier, Y., Dubois, P. M., and Fusco, A. (1992) *Br. J. Cancer* **66,** 1094–1098
77. Nikiforov, Y. E., Rowland, J. M., Bove, K. E., Monforte-Munoz, H., and Fagin, J. A. (1997) *Cancer Res.* **57,** 1690–1694
78. Ito, T., Seyama, T., Iwamoto, K. S., Hayashi, T., Mizuno, T., Tsuyama, N., Dohi, K., Nakamura, N., and Akiyama, M. (1993) *Cancer Res.* **53,** 2940–2943
79. Nikiforov, Y. E., Koshoffer, A., Nikiforova, M., Wang, J., Stringer, J., and

Fagin, J. A. (1999) *Oncogene*, in press
80. Hall-Jackson, C. A., Jones, T., Eccles, N. G., Dawson, T. P., Bond, J. A., Gescher, A., and Wynford-Thomas, D. (1998) *Br. J. Cancer* **78,** 641–651
81. Pitti, R. M., Marsters, S. A., Lawrence, D. A., Roy, M., Kischkel, F. C., Dowd, P., Haung, A., Donahue, C. J., Sherwood, S. W., Baldwin, D. T., Godowski, P. J., Wood, W. I., Gurney, A. L., Hillan, K. J., Cohen, R. L., Goddard, A. D., Botstein, D., and Ashkenazi, A. (1998) *Nature* **396,** 699–703

Involvement of Protein Kinase Cε (PKCε) in Thyroid Cell Death: A TRUNCATED CHIMERIC PKC ε CLONED FROM A THYROID CANCER CELL LINE PROTECTS THYROID CELLS FROM APOPTOSIS

Jeffrey A. Knauf, Rosella Elisei, Daria Mochly-Rosen, Tamar Liron, Xiao-Ning Chen, Rivkah Gonsky, Julie R. Korenberg and James A. Fagin

Access the most updated version of this article at http://www.jbc.org/content/274/33/23414

Alerts:
- When this article is cited
- When a correction for this article is posted

Click here to choose from all of JBC's e-mail alerts

This article cites 80 references, 35 of which can be accessed free at
http://www.jbc.org/content/274/33/23414.full.html#ref-list-1